Mapping inundation from sea level rise and its interaction with land cover in the Sundarbans mangrove forest

Akbar Hossain Kanan[1] · Francesco Pirotti[1,2] · Mauro Masiero[1] ·
Md Masudur Rahman[3]

Abstract

The sea level rise (SLR) in the Sundarbans areas is higher than the global-average rate of sea rise, and many studies assume that most of the dry land of the Sundarbans will be inundated by the end of the twenty-first century. This study aims to analyze the amount of dry land that can potentially be inundated by SLR in Sundarbans and the impact under different land cover conditions. Four SLR scenarios, a digital elevation data grid, and net subsidence data are used to map areas that will be potentially inundated by 2100. Results for the low (35 cm), mid (52 cm), high (70 cm), and extreme (147 cm) SLR scenarios indicate that the Sundarbans landmass area will be flooded up to 40 km^2 (1%), 72 km^2 (1.8%), 136 km^2 (3.4%), and 918 km^2 (23%), respectively, under the current net subsidence rate of −2.4 mm/year by 2100. Except for the extreme scenarios, the low, mid, and high SLR will result in riverbank and beach areas to be covered by water. The potential inundation areas of different vegetation cover classes that already exist today (2020) will be nominal for the low, mid, and high SLR scenarios. We also analyzed the sensitivity of the results through station-based SLR data, which fits with the low (35 cm) SLR scenarios under the −2.4 mm/year subsidence rate. This study concluded that the inundation aspect of SLR will not directly affect the Sundarbans; however, indirectly related threats and anthropogenic disturbances can be major drivers of the Sundarbans' degradation by the end of the twenty-first century. This work discusses reasonable inundation scenarios integrating SLR and subsidence with a custom land-cover map that includes three forest-density categories. The study's findings contribute to forest management planning and support the UN goals of the Bangladesh Delta Plan.

Keywords Sundarbans mangrove · Land cover · Inundation · Sea level rise · Digital elevation models · Subsidence

1 Introduction

Sundarbans is the single largest continuous productive mangrove forest in the world (Ghosh et al. 2015), offering a wide range of ecosystem services (FAO 2010). According to the 2011 census data, about 3.5 million Bangladeshi people are directly or indirectly

dependent on these ecosystem services for livelihood and socio-economic well-being (Kibria et al. 2018; Ortolano et al. 2016; Roy et al. 2013; Giri et al. 2007), but the number of people depending on Sundarbans is still increasing (Ghosh et al. 2015). Most importantly, Sundarbans protect coastal communities and their properties from storms, cyclones, and coastal soil erosion. Moreover, Sundarbans host many threatened and endangered species (e.g., Bengal tiger: *Panthera tigris tigris*) (Ortolano et al. 2016). The carbon sequestration rate of mangrove forests is four times higher than other tropical forests (Donato et al. 2011); consequently, Sundarbans contribute significantly to reducing greenhouse gas emissions. Recognizing the significance and uniqueness of Sundarbans, the United Nations Educational, Scientific and Cultural Organization (UNESCO) declared it a World Heritage Site in 1997 (Quader et al. 2017). Before this, it was included as a Ramsar site in 1992 (Rahman et al. 2015). Despite their importance, the area and biodiversity of the Sundarbans are decreasing at an alarming rate due to both anthropogenic activities and climate change-related factors (Islam et al. 2020; Sannigrahi et al. 2020; Neogi et al. 2017).

Climate change, particularly the associated sea level rise (SLR), is considered a severe threat to the coastal region, including the Sundarbans of Bangladesh (Jabir et al. 2021; Islam et al. 2016). The reason is that the SLR in Sundarbans regions is much higher (3.90 ± 0.46 mm/year) (Nishat et al. 2019) than the rate of global-average sea rise (1.8 ± 0.5 mm/year) (Deb and Ferreira 2017; Karim and Mimura 2008). Jabir et al. (2021) reported that a SLR of 10 cm, 25 cm, 45 cm, and 60 cm will inundate 15%, 40%, 75%, and 100% of the Sundarbans, respectively. Colette (2007) reported that a 45 cm rise in the global sea level by 2100 might lead to the destruction of 75 % of the Sundarbans. A study by the World Bank (2000) predicted that a SLR rise by 1.0 m will destroy most of the Sundarbans. However, Brammer (2014) reported that there is a common misperception that the situation in Bangladesh's coastal region will worsen due to the rising sea level in the twenty-first century. Brammer highlights the following limitations of present studies: (i) the assumptions and descriptions forecasting destructive inundation effects of the Sundarbans due to the SLR are largely incorrect; (ii) the potential inundation level and its impacts on the Bangladesh coastal area (including Sundarbans) due to SLR in the twenty-first century is still unclear; (iii) the adoption of appropriate measures based on knowledge of the physical geography are not accounted for; and (iv) rates of coastal erosion and subsidence rates do not account for variability and dynamicity of Bangladesh coastal areas.

The study on the future inundation of Sundarbans is essential to clarify the assumption and inform future forest management strategies. However, a few studies have been completed with remarkable limitations. Loucks et al. (2010) estimated that tiger habitat in Bangladesh's Sundarbans would decline by 96% from inundation if SLR increases by 28 cm in 2070. In their estimation, they did not consider the subsidence rate which significantly influences calculations of the future inundation of Sundarbans (Brammer 2014). Similarly, Lovelock et al. (2015) projected inundation based on mean sea level (MSL) rise and did not consider tides, sedimentation, and subsidence. Payo et al. (2016) and Ghosh et al. (2019) estimated future inundation levels considering the subsidence, but they did not provide information on how they used subsidence value to compute inundation. Furthermore, they applied the IPCC projections under the Representative Concentration Pathway (RCP) 4.5 and 8.5 scenarios of West Bengal of India to find possible inundation of Bangladesh Sundarbans. However, the SLR projection for the RCP 4.5 and 8.5 scenarios for West Bengal and Bangladesh Sundarbans is different. Mukul et al. (2019) projected SLR impacts on Bengal tiger habitats in the Bangladesh Sundarbans in 2070 using the Shuttle Radar Topography Mission (SRTM) data. However, SRTM data is associated with a significant vertical error (Al-Nasrawi et al. 2021), and the error increases for densely vegetated areas (Kulp and Strauss 2016). Moreover, Mukul et al. (2019) did not consider the subsidence of Sundarbans, which is an essential

variable for calculating future inundation (Brammer 2014). Research on inundation effects using the "Forest And Buildings removed Copernicus Digital Elevation Model" (FABDEM) in the Sundarbans is not ideal as only 55% of forest pixels have an error lower than 2 m elevation (Hawker et al. 2022). However, 36% of the lands of Sundarbans are less than 2 m from the mean sea level (Supplementary Fig. 2). None of the aforementioned studies used the station-based SLR data of Sundarbans to compare the differences with IPCC projection. In addition, no studies have been found regarding the SLR impact on the land cover of Sundarbans in the future. These uncertainties in present literature have motivated this study. In our study research, we tried to overcome the limitations of existing studies by careful investigation of data collection, data processing, and validation, which is a prerequisite to predicting future inundation and its impact. Therefore, this study aims to map the potential inundated and impacted areas with three different forest land cover classes (dense, moderate, and sparse forest) of Sundarbans due to SLR by the end of the twenty-first century.

2　Description of study area

The present study considered the Bangladesh Sundarbans Mangrove forest, which is located between 21°30′ and 22°30′ N and 89°00′ and 89°55′ E, covering 6200 km^2 (Ghosh et al. 2015) (Fig. 1). The Sundarbans are formed on the estuary created by the Hooghly, Ganges, Brahmaputra, and Meghna rivers in the Bay of Bengal. These rivers are the key sources that supply fresh water and sediments to Sundarbans. The average elevation of the forest floor is about 2 m above mean sea level (Payo et al. 2016). Approximately 30% of areas of the Sundarbans are covered by water due to numerous rivers, canals, and tidal flows (Nishat et al. 2019). The tide inundates the forest twice a day (Barlow et al. 2011). The area is characterized by a tropical climate with a dry season from December to February and a monsoonal wet season from March to November (Quader et al. 2017). Seasonal mean minimum and maximum temperatures vary from 12 to 24°C and from 25 to 35°C, respectively. The total annual amount of precipitation is between 1500 and 2000 mm. Tropical cyclones always make landfall in the Sundarbans during the monsoon season, causing severe flooding and wind damage to the forests (Ghosh et al. 2015).
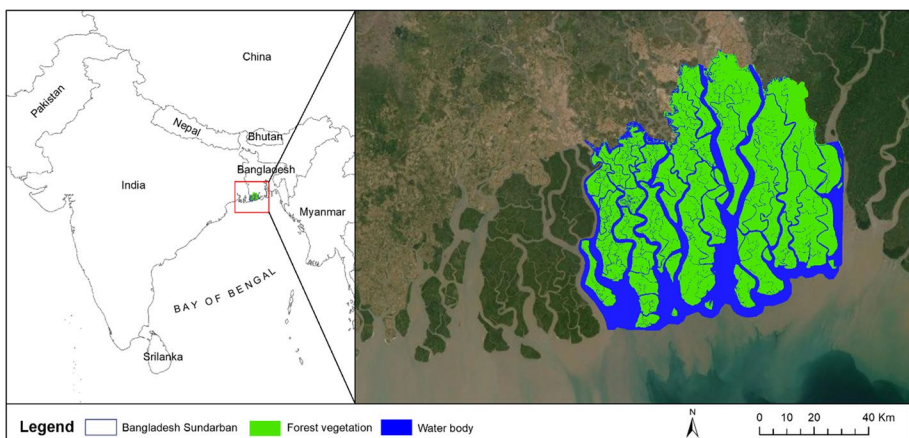

Fig. 1 Sundarbans mangrove forest (study area)

3 Methodology

Geospatial data were used to assess the future inundation level and impacted land cover areas of the Bangladeshi Sundarbans. Adopted methodological steps consisted of the following: (i) data collection and processing, (ii) calculation of inundation to generate the scenarios, and (iii) geospatial modelling of future inundation level and impacted land cover areas. The input data include the following: (i) digital elevation model (DEM) from 1991 from the Water Resources Planning Organization (WARPO) at 50 m spatial resolution with 0.5 m accuracy (1σ), (ii) three subsidence rate scenarios +2.4 mm/year, 0 mm/year, −2.4 mm/year (Brown and Nicholls 2015); (iv) four SLR scenarios from IPCC, 35 cm, 52 cm, 70 cm, and 147 cm; (v) one SLR scenario of 29 cm from station data; and (vi) Landsat satellite images of Sundarbans area at 30 m spatial resolution—see supplementary Table 1. The DEM refers to elevation of the terrain without vegetation or above-ground structures. Elevation data is a key assumption that drives results, and is described in detail in the next section.

3.1 Data collection and processing

3.1.1 Digital elevation model

The points used for creating the DEM that was used in this study were collected from the Water Resources Planning Organization (WARPO). The survey and DEM for Sundarbans were generated by a Finnish consulting firm (FINNMAP) in 1991 for the Bangladesh government, measuring elevation above sea level for 80,584 points using GNSS (Ghosh et al. 2019; Loucks et al. 2010). The original FINNMAP data were georeferenced to the Survey of Bangladesh datum (SOB), which is a stable datum representing the present mean sea level (MSL). According to Payo et al. (2016), the Institute of Water Modelling (IWM) Bangladesh restructured the DEM data using Google images from 2006 to 2007 to rectify outdated FINNMAP elevation data. This new data was resampled at a resolution of 30 m and released to the Public Works datum (PWD), which has been established by the Bangladesh government at 0.459 m below MSL (Payo et al. 2016). Based on the WARPO data, we generated an elevation map of Sundarbans for this study (Supplementary Fig. 1), using the PWD datum. The vertical resolution of the DEM data is expressed in centimeters ranging from 0 to 400+ cm (max 608 cm). We found that 4% of the area remains at >0 to 100 cm elevation. Most of the Sundarbans area (73%) belongs to 151 to 300 cm elevation (Supplementary Fig. 2), and the average elevation is 200 cm (2 m) from MSL. This DEM is a reference for several studies and has been defined as the main source of elevation data (World Bank 2010): "the main source of topographic elevation data for the coastal region of Bangladesh is the FINNMAP land survey, FAP 19- National DEM (1952-64), and projects of the Bangladesh Water Development Board (i.e., Khulna Jessore Drainage Rehabilitation Project, 1997; Beel Kapalia project, 2008; and Beel Khuksia project, 2004)." The FINNMAP topographic maps and other data were digitized to develop a digital elevation model (DEM) of the coastal region of Bangladesh. The grid size of the model is 50 m × 50 m.

It must be noted that we assume the elevation values in the DTM to be consistent with the documentation of the data; e.g., points were surveyed on the ground with state-of-the-art topographic surveys and GNSS. The expected error of the elevation of the points surveyed on the ground reasonably falls in an envelope of ±50 cm (1σ). Points surveyed with GNSS receivers or classical triangulation usually reach higher accuracy, but to be

conservative, we will assume that to be the expected accuracy. The interpolation procedure to create the grid will increase slightly this figure, to reach the < 1 m value mentioned in Payo et al. (2016). It is also true that the scale and resolution of the raster, 50 m pixel resolution, is such that the intra-pixel elevation variance can be higher than the accuracy, as terrain roughness in a 50 m × 50 m area can reasonably lead to higher variability. We agree that this uncertainty propagates to the results, but argue that this product is what is best available, also considering that past and recent studies have either used this product or less accurate data. On these arguments, we hold true the following two assumptions: (1) 50 cm is the conservative estimation of the accuracy of the center of each cell in the WARPO DEM; i.e., the elevation value at the pixel is inside a ±0.5-m envelope that represents ~68% probability of the real value falling inside that interval; and (2) we are expecting this uncertainty to be randomly distributed across pixels, without any spatial autocorrelation. The results and discussion in this paper report scenarios that are consistent with the above-stated assumptions. An improved digital elevation model with higher accuracy, with today's technologies, can be obtained with a LiDAR survey across the study area, but that is not available at the time of writing.

3.1.2 Subsidence rate

The Sundarbans is located in the Ganges–Brahmaputra–Meghna (GBM) basin, which lies in the largest active delta of the world (Paszkowski et al. 2021). For this reason, land subsidence and land rise are common phenomena, resulting in changes of the land elevation with respect to MSL. Land subsidence in deltas is due to tectonics, compaction, reduced sedimentation, and other anthropogenic activities (e.g., groundwater withdrawal, mining, dam construction, and deforestation) (Syvitski et al. 2009). The net subsidence is the difference between land sinking and land rising: it could be downward (sinking > rising), upward (sinking < rising), or level (sinking = rising). The land sinking and rising of Sundarbans are shown in Fig. 2: the net subsidence of Sundarbans is downward, implying the inundation level should be increased (Brown and Nicholls 2015). The calculation of the subsidence rate for the Sundarbans between two periods is calculated according to the Eq. (1).

$$SR_{(t_1 - t_2)} = LS - LR \tag{1}$$

where SR = subsidence rate, $t_1 - t_2$ = time difference, LS = land sinking, LR = land rising

In this study, we considered net subsidence rates based on Brown and Nicholls (2015), who reviewed Ganges–Brahmaputra–Meghna (GBM) net subsidence rates, reporting 205 measurements based on a range of methods and timescale. They found that the Sundarbans have the lowest net subsidence rate with a mean value of −2.8 mm/year and a median value of −2.0 mm/year compared to other land uses of this delta. The lowest net subsidence rate in the Sundarbans might be due to the final destination of sediment deposition from upstream flow and low soil compaction. Brown and Nicholls (2015) concluded that the median subsidence rate was preferable to the mean since a few big single subsidence measurements influenced the results. Therefore, a representative value of −2.4 mm/year of net subsidence rate in the Sundarbans was used in this study (Ghosh et al. 2019). In our model, we also used +2.4 mm/year and 0.0 mm/year to assess the sensitivity of the results to the uncertainty of the net subsidence rate.
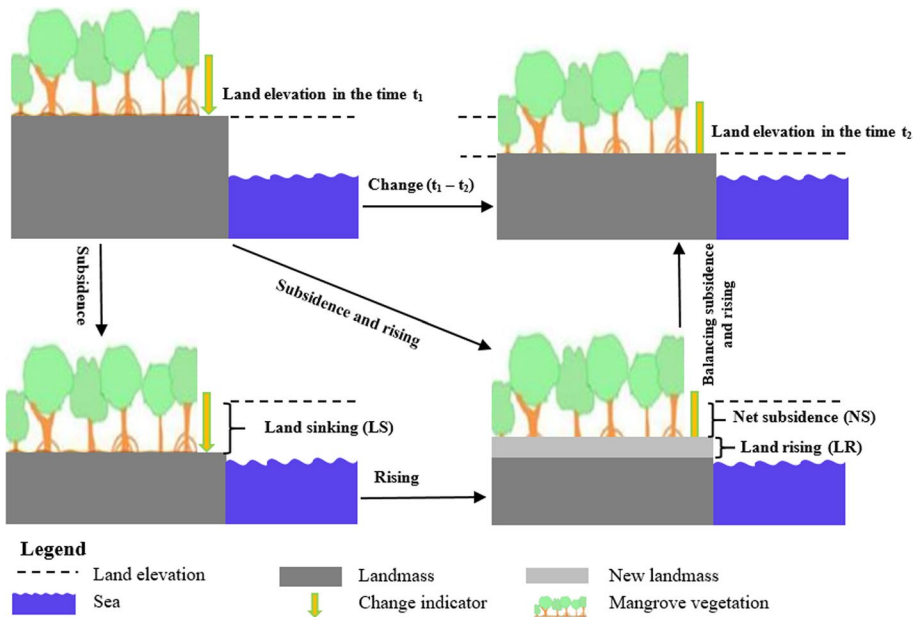
Fig. 2 Land sinking, rising, net subsidence of Sundarbans

3.1.3 Sea level rise

We collected IPCC (RCP 4.5 and 8.5) global projected and station-based measured SLR data (Hiron Point) to understand the possible inundation level in Sundarbans by the end of the twenty-first century. The low and mid sensitivity under the RCP 8.5 scenario is almost similar to the high and mid sensitivity under RCP 4.5 (Fig. 3a and b). Moreover, analysis of station-based data from 1977 to 2020 showed that the sea level is increasing in Sundarbans according to a + 0.36 cm/year annual rate (Fig. 3c). By the end of the twenty-first century, the SLR would be 29 cm (Fig. 3d), close to the RCP 4.5 low sensitivity (Fig. 3a). Therefore, four different SLR scenarios of 35 cm (low), 52 cm (mid), 70 cm (high), and 147 cm (extreme) were considered for this study (Fig. 3d). The 35 cm, 52 cm, and 70 cm SLR are, respectively, based on the low, mid, and high projections under the IPCC RCP 4.5 scenario for Sundarbans regions (Ghosh et al. 2019; Payo et al. 2016). The extreme case scenario is like the H++ scenario range, which considers the 95 percentile value for RCP 8.5 (97 cm) plus 50 cm associated with Antarctic ice-sheet melting (Levermann et al. 2014; Lovelock et al. 2015). The extreme case scenario is considered possible but unlikely (Jevrejeva et al. 2014).

3.1.4 Land cover from Landsat 8 image analysis

Satellite open data provides the means to assess effects of forest disturbance across large areas (Vaglio Laurin et al. 2020). Radiometrically and geometrically calibrated (Level 2) Landsat-8 images at ~30 m resolution were retrieved from Earth Explorer (https://earthexplorer.usgs.gov/) and used in this study to identify the land cover classes over
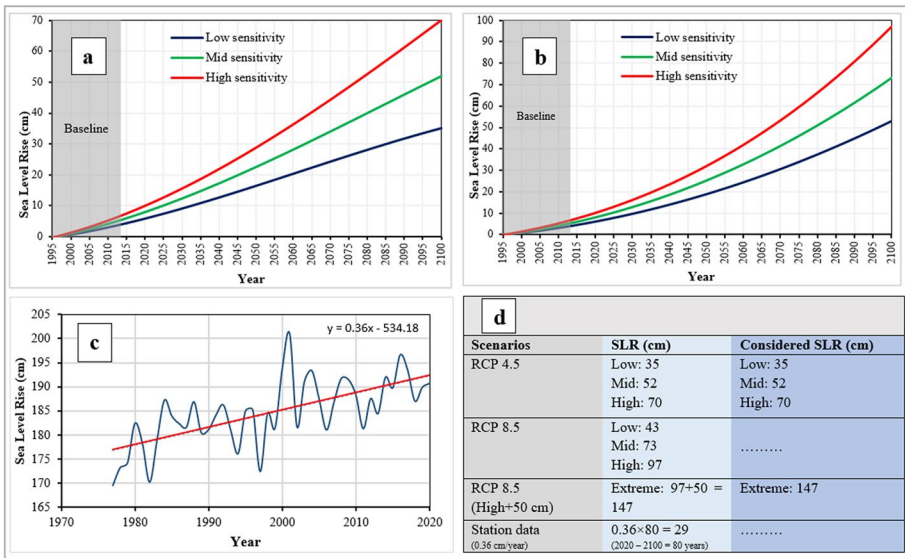
Fig. 3 **a** IPCC projection of SLR under the RCP 4.5 scenario; **b** IPCC projection of SLR under the RCP 8.5 scenario; **c** SLR of Sundarbans based on station data (Hiron point); **d** SLR values from different scenarios considered in the study

Sundarbans. Satellite images provide the surface reflectance (unitless) which is a measure of the fraction of incoming solar radiation that is reflected from the Earth's surface to the Landsat sensor.

A supervised classification using maximum likelihood (ML) algorithm was used to classify the study area with five labels: dense forest, moderate forest, sparse forest, barren land, and water body. The supervised ML algorithm has been used worldwide over the past two decades to study mangrove land cover (Kumar et al. 2021; Islam et al. 2019; Bera and Chatterjee 2019; Jones et al. 2016; Ghosh et al. 2016; Pham and Yoshino 2015; Chen et al. 2013; Rahman 2013; Giri et al. 2010). An appropriate number of training samples is a prerequisite for a successful and accurate land cover classification (Lu and Weng 2007). We manually selected 200 training samples by careful inspection of homogenous pixels of the five different land cover classes using high-resolution Google Earth images as a reference to identify the existing land cover for year 2020. The training samples were stratified among the selected land cover classes as follows: 40 samples for dense forest, 40 for moderate dense forest, 35 for sparse forest, 30 for barren land, and 55 for water bodies. The water color varies near the coastal/beach/shoreline areas than the deep river basins of Sundarbans due to the sedimentation, water deepness, and tidal effect; thus, the spectral variation is slightly different (Akbar Hossain et al. 2022). In this case, we considered many water body sites for training samples.

For the accuracy assessment, we randomly sampled an independent set of 200 control points with the same stratification over the five classes using the classified images and validated them using Google Earth historical images. The classification accuracy was assessed by computing error metrics (producer, user, and overall accuracy) and kappa coefficient (Kanniah et al. 2015; Stehman 1996). The overall accuracy and kappa

coefficient were 91% and 0.86, respectively (Table 1), which indicates an acceptable degree of accuracy in the resulting land cover classification. After the accuracy assessment, we completed the final map for 2020 (Supplementary Fig. 3). The study found that the dense, moderate, and sparse forests are 25%, 24%, and 17%, respectively. The largest LULC class corresponds to water bodies (33%), and fewer areas (2%) are barren land (Supplementary Fig. 4).

3.2 Calculation of inundation to generate the scenarios

The inundation of Sundarbans is not only associated with SLR but also subsidence. If the subsidence rate is negative (i.e., lower than zero), then it must be added to the global SLR to estimate the inundation level. In the case of zero subsidence, no need to add, while if the subsidence rate is positive (i.e., higher than zero), it must be subtracted from the global SLR (Brammer 2014). Therefore, our model adjusted the SLR and subsidence rate to calculate inundation level, according to the following equations.

$$IUL_{(S)} = SLR_{(G)} + \left(SR_{(y)} \times t\right) \quad \left[if, subsidence\ rate < 0\right] \tag{2}$$

$$IUL_{(S)} = SLR_{(G)} \quad \left[if, subsidence\ rate = 0\right] \tag{3}$$

$$IUL_{(S)} = SLR_{(G)} + \left(-SR_{(y)} \times t\right) \quad \left[if, subsidence\ rate > 0\right] \tag{4}$$

where $IUL_{(S)}$ = inundation level of Sundarbans, $SLR_{(G)}$ = global sea level rise (IPCC), $SR_{(y)}$ = subsidence rate, and t = time difference between elevation data collection and future projection (e.g., 2100−1991 = 109 years).

After calculating the inundation level, the twelve scenarios were developed using different SLR and subsidence rate to find out the potential inundated and affected land cover areas of Sundarbans by the end of the century (Table 2).

3.3 Mapping future inundation and land cover change

A simple deterministic bathtub model was applied to map potential inundation levels. In this method, the water level is simply raised on a coastal DEM by selecting all areas below the desired new water level height to identify the inundation zone (Anderson et al. 2018). This bathtub method (stated to as a "zero-side rule") does not consider surface connectivity at all between grid cells and is widely used to predict and assess coastal flooding due to SLR (Poulter and Halpin 2008; Gesch 2018). The calculated inundation values (see Section 3.2) were spatially processed by combining the four different SLR values (35 cm, 52 cm, 70 cm, and 147 cm) and the three subsidence rates (−2.4 mm/year, 0.0 mm/year, and +2.4 mm/year). Twelve raster files resulted from this process. Raster data were then converted to a vector model to map the twelve SLR scenarios. Finally, these twelve SLR scenarios were overlaid on the land cover base map (from the year 2020) to assess the potential impact of inundation levels on the different land cover classes by the end of the twenty-first century (Supplementary Fig. 5).

Table 1 Analysis accuracy metrics of classified Landsat images of Sundarbans (2020); "PA" and "UA" indicates producer's and user's accuracy respectively

Year (used sensor)	Land cover classes										Overall accuracy (%)	Kappa coefficient (K)
	Dense forest		Moderate dense forest		Sparse forest		Barren land		Water body			
	PA (%)	UA (%)	PA (%)	UA (%)	PA (%)	UA (%)	PA (%)	UA (%)	PA (%)	UA (%)		
2020 (OLI-TIRS)	89.2	90.7	87.1	88.0	89.1	86.8	80.9	89.4	96.6	93.7	91.0	0.86

Table 2 Twelve scenarios using different SLR and subsidence rate

SLR (cm)	Net subsidence		
	−2.4 mm/year	0 mm/year	+2.4 mm/year
35	Scenario: 1	Scenario: 2	Scenario: 3
52	Scenario: 4	Scenario: 5	Scenario: 6
70	Scenario: 7	Scenario: 8	Scenario: 9
147	Scenario: 10	Scenario: 11	Scenario:12

4 Results

4.1 Landmass inundation in future SLR scenarios and net subsidence

The results of the SLR models indicate that the potential inundation of the Sundarbans area by the end of the twenty-first century will be minimal for the low (35 cm), mid (52 cm), and high (70 cm) SLR scenarios and significant for the extreme (147 cm) SLR scenario (Fig. 4). The potential inundation areas under the −2.4 mm/year net subsidence rate are predicted to be higher for low, mid, high, and extreme SLR scenarios than under the other two net subsidence rates considered for the study (Fig. 5). The map in Fig. 5 shows that, except for the extreme scenario, the low, mid, and high SRL will inundate the few areas of riverbank, beaches, and islands.

The Sundarbans landmass area is projected to be inundated by 40 km^2 (1%), 72 km^2 (1.8%), and 136 km^2 (3.4%) by the end of the twenty-first century for the low, mid, and high SLR scenarios, respectively, under the current net subsidence rate of −2.4 mm/year (Table 3). The results indicate a maximum of 918 km^2 (23%) landmass area will be inundated under the extreme SLR and a −2.4 mm/year. However, landmass inundation will
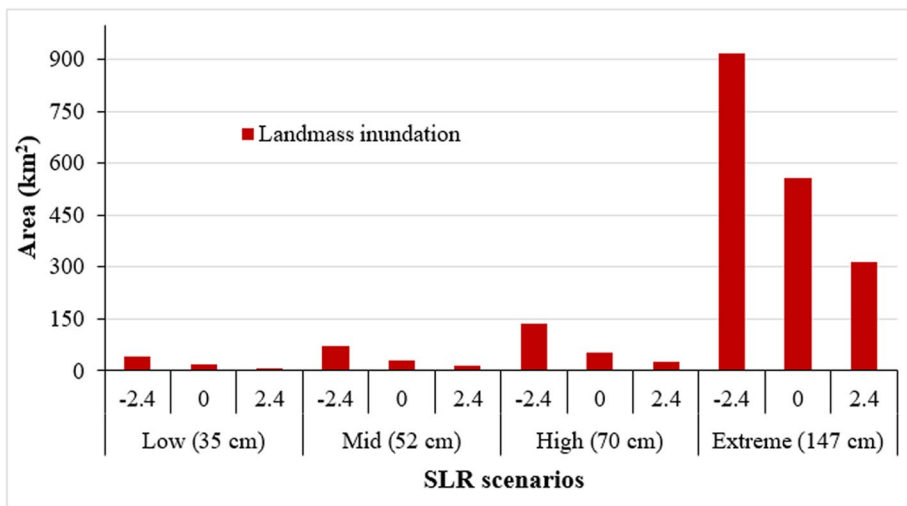

Fig. 4 Potential inundation of landmass areas under different SLR scenarios (cm) and net subsidence (mm/year) in 2100
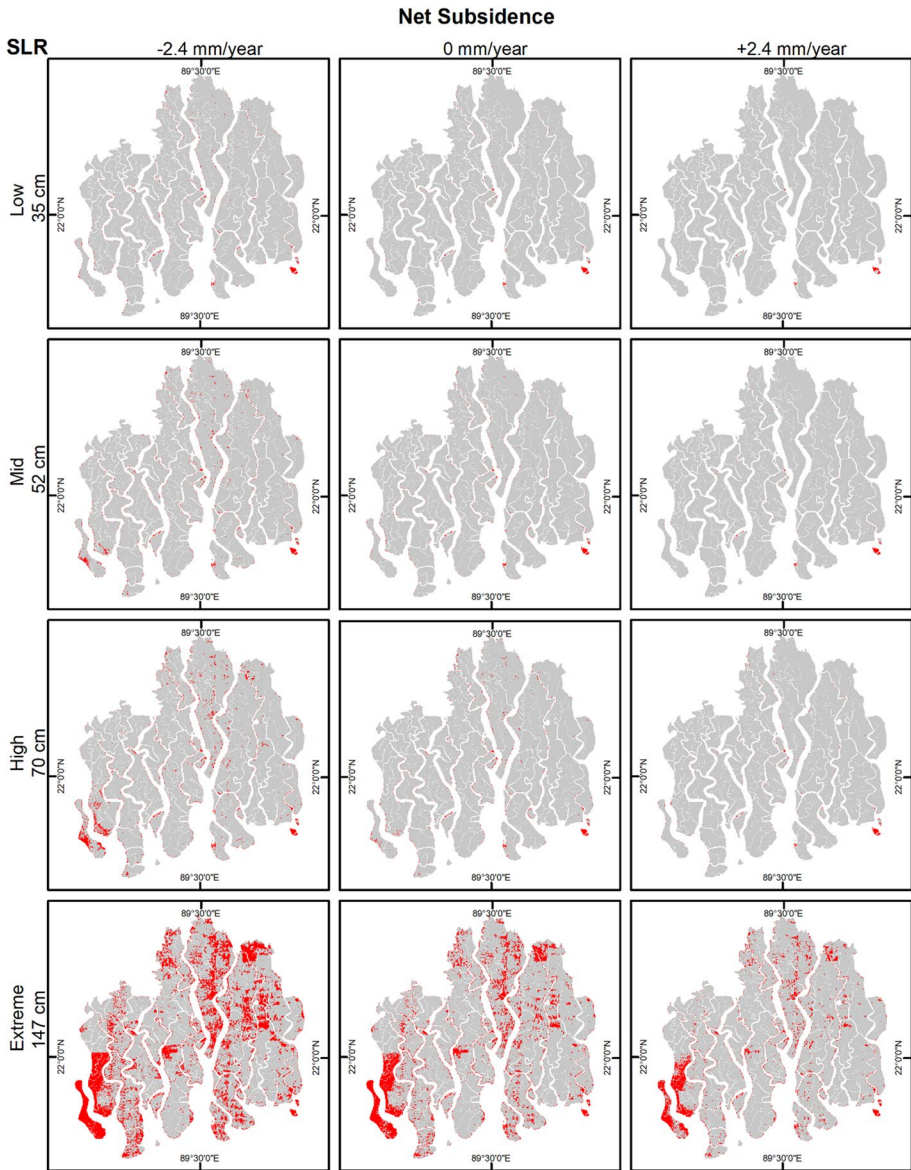
Fig. 5 Potential inundation areas under future (2100) SLR scenarios and net subsidence

decrease under 0 mm/year and the +2.4 mm/year net subsidence rates for all SLR scenarios. The results of the model show that the potential inundation areas will be located disjointly for the low (35 cm), mid (52 cm), and high (70 cm) SLR scenarios. However, the inundation areas will be more adjacent and continuous under the extreme SLR scenario, and the north-east and south-east parts of the Bangladesh Sundarbans will be highly affected (Fig. 5).

Table 3 Analysis of possible landmass inundation under different SLR scenarios and net subsidence (NS) in 2100

Landmass inundation	SLR 35 cm			SLR 52 cm			SLR 70 cm			SLR 147 cm		
	NS mm/year			NS mm/year			NS mm/year			NS mm/year		
	−2.4	0	+2.4	−2.4	0	+2.4	−2.4	0	+2.4	−2.4	0	+2.4
km^2	40	19	6	72	31	14	136	54	25	918	555	316
%	1	0.5	0.2	1.8	0.8	0.3	3.4	1.3	0.6	23	14	8

4.2 Impacted land cover fraction

The results of the simulated model show that the potential inundation areas of different land cover classes by the end of the twenty-first century will be limited for the low, mid, and high SLR scenarios (Fig. 6). The highest potential inundation is found for the barren lands, followed by moderate dense forest, sparse forest, and dense forest for all SLR scenarios. The study indicates that 5 km^2, 12 km^2, and 28 km^2 dense forest will be reduced for the low, mid, and high SLR scenarios, respectively, under the −2.4 mm/year subsidence rate (Table 4). At the same time, 19 km^2, 28 km^2, and 41 km^2 barren land will be decrease for the same SLR scenarios and subsidence rate. In the case of the extreme SLR, the inundated areas will be higher than the other three SLR scenarios, resulting in larger forest areas being inundated than the barren land (Table 4). The results of the model show that the potential inundation of dense, moderate dense, sparse, and barren land areas will be higher for low, mid, high, and extreme SLR scenarios under −2.4 mm/year subsidence rate than the other two subsidence rates (Fig. 7).
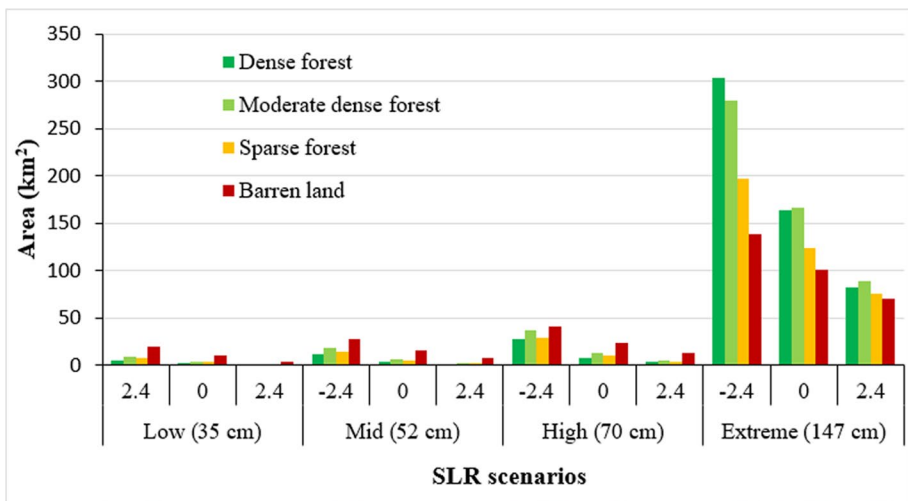

Fig. 6 Potential inundation of land cover classes under different SLR scenarios (cm) and net subsidence (mm/year) in 2100

Table 4 Analysis of possible impacted area (km^2) of land cover classes under different SLR scenarios and net subsidence (NS) in 2100; *DF* dense forest, *MDF* moderate dense forest, *SF* sparse forest, *BL* barren land

Land cover inundation (km^2)	SLR 35 cm			SLR 52 cm			SLR 70 cm			SLR 147 cm		
	NS mm/year			NS mm/year			NS mm/year			NS mm/year		
	−2.4	0	+2.4	−2.4	0	+2.4	−2.4	0	+2.4	−2.4	0	+2.4
DF	5	2	0.27	12	4	1	28	8	3	304	164	82
MDF	9	4	0.82	18	6	2	37	13	5	280	166	89
SF	7	3	0.78	14	5	2	29	10	4	197	124	75
BL	19	10	4	28	15	8	41	23	13	138	101	70

5 Discussion

5.1 Accuracy of elevation values for modelling future inundation

The DEM data significantly influences the calculation of potential inundation due to SLR. In this study, we used 50 m resolution DEM data, which was first created by a Finnish consulting firm (FINNMAP), measuring 80,584 GPS elevation points in millimeters (mm) above sea level in 1991 (Ghosh et al. 2015). Therefore, the accuracy is higher than the SRTM and FABDEM, which have not been used in previous studies. However, the WARPO DEM has an uncertainty of 50 cm expressed as a standard deviation (1σ), which is a higher value than some of the scenarios in the study. The error in DEM values is considered to be unbiased and normally distributed, without any spatial autocorrelation. This assumption is done because we have a global measure of the vertical accuracy and not the full reference dataset to allow analysis of correlation on residuals. This implies using a deterministic approach to define the envelope around values (Gesch 2018) and is a limitation that cannot be resolved without further ground measurements. The estimated effect of SLR must be compared with a confidence value which is related to the value of SLR normalized with the standard deviation of the DEM, which is the same as the RMSE according to our assumptions. Gesch (2018) shows how express the confidence of the contour line that delimits the flooded area as a function of the DEM accuracy metrics. The 68% confidence is given by twice the RMSE, thus in our case ±50 cm. We can reverse the process and find the confidence for the values of the SLR scenarios to be included in an interval that has the same range as the SLR value for that scenario. This results in the 35 cm, 52 cm, and 70 cm SLR scenarios to have the line that separates inundated and non-inundated land, respectively, with a 27%, 40%, and 52% expected probability to be placed vertically within an interval, respectively, of ±17.5 cm, ±26 cm, and ±35 cm of the true location. The inundated levels at the 147 cm SLR scenario have a higher confidence of 86% that the inundation line is placed vertically within ±73.5 cm of its true location. The practical impact of these confidence levels of vertical position of water levels is that the results reported in this study, just like other studies, are strongly dependent on DEM accuracy, thus advocating for more efforts in investment in technology for better global DEMs.

Regarding subsidence rates, we considered a net subsidence rate of −2.4 mm/year based on Brown and Nicholls (2015), who reviewed net subsidence rates, reporting 205 measurements based on a range of methods and timescales. The Sundarbans is located within the largest and populous delta in the world (Paszkowski et al. 2021). Therefore, land subsidence and rising are common phenomena, resulting in the change in the land elevation to
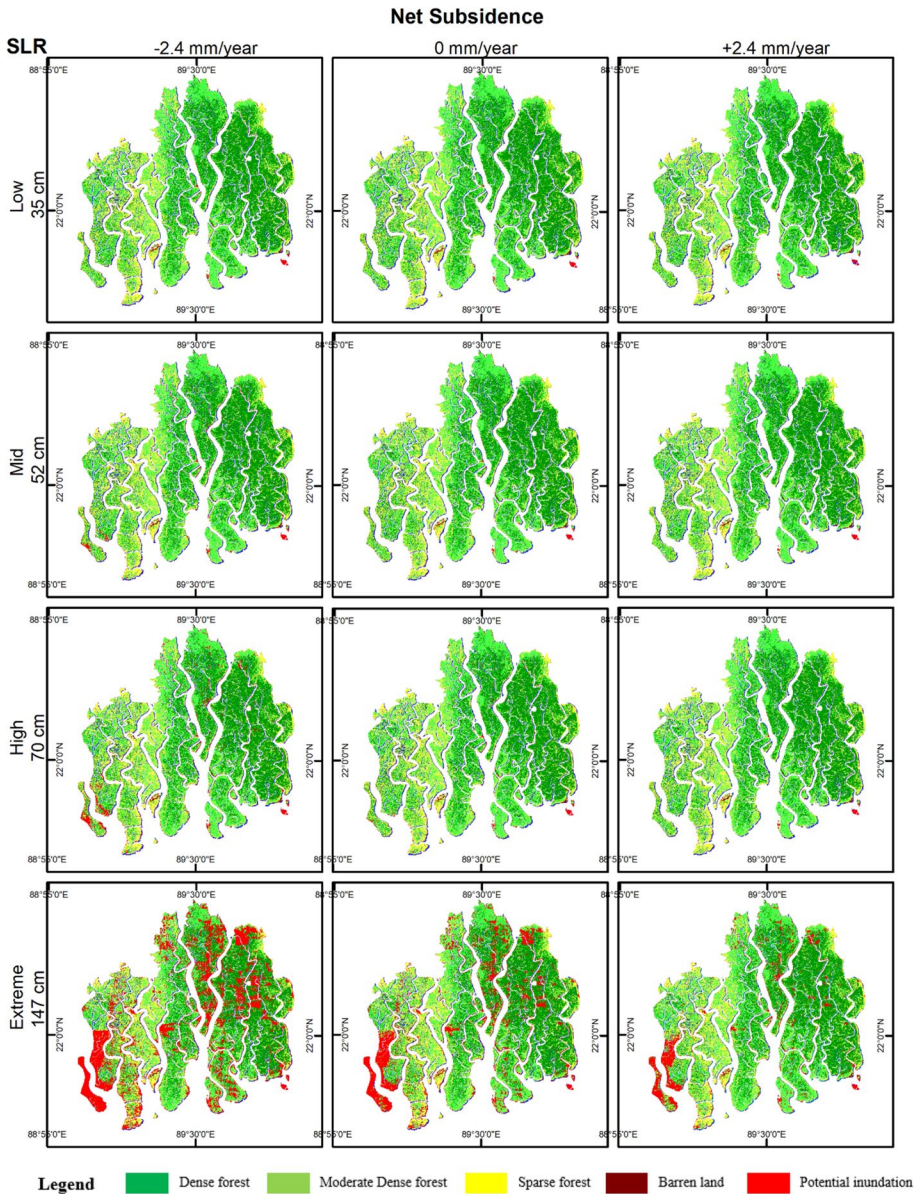
Fig. 7 Potential inundation of different land cover classes under future (2100) SLR scenarios and net subsidence overlapped with the current (2020) land cover classes

MSL over time. For this reason, we analyze the sensitivity of the results by considering subsidence rates of 0 mm/year and +2.4 mm/year. This study showed twelve possible inundation scenarios under different SLR (IPCC) and subsidence rates for the twenty-first century. In addition, we justified the model using station-based SLR data of Bangladesh Sundarbans, which might increase the prediction accuracy for the potential inundation scenario.

5.2　Potential landmass inundation due to future scenarios

According to our results, the potential landmass inundation of the Sundarbans due to SLR by the end of the twenty-first century could be much lower than the assumption has been in the last few decades. For instance, Jabir et al. (2021) reported that 75% of Sundarbans will be inundated by 45 cm SLR. Similarly, Colette (2007) suggested that a 45 cm rise in global sea level by 2100 might lead to the destruction of 75% of the Sundarbans. In addition, the SLR rise by 100 cm (1.0 m) will destroy the entire Sundarbans (World Bank 2000). However, our model indicates that a SLR of 35 cm, 52 cm, and 70 cm under the current subsidence rate (−2.4 mm/year) will inundate 1%, 1.8%, and 3.4% landmass of Sundarbans, respectively. The result shows that a maximum of 23% of landmass will be inundated by 147 cm SLR and a −2.4 mm/year net subsidence rate. Except for the extreme case scenarios, the low, mid, and high SLR under −.4 mm/year subsidence rate will inundate the riverbanks and beaches (Fig. 8). The extreme case scenario is considered possible but unlikely (Jevrejeva et al. 2014). Moreover, our study's elevation distribution graph (Supplementary Fig. 2) shows that only 4% area of Sundarbans remains at >0 to 100 cm elevation, and 32% belongs to 101 to 200 cm elevation. The findings of our study are different from those reported by previous studies (e.g., Jabir et al. 2021; Colette 2007; World Bank 2000) as they rely on various assumptions; this raises concerns about the assumptions of previous studies and ultimately questions their results. According to Brammer (2014), there is a general misconception that the situation in the coastal areas of Bangladesh (including Sundarbans) will deteriorate by the end of the twenty-first century due to SLR. The same author
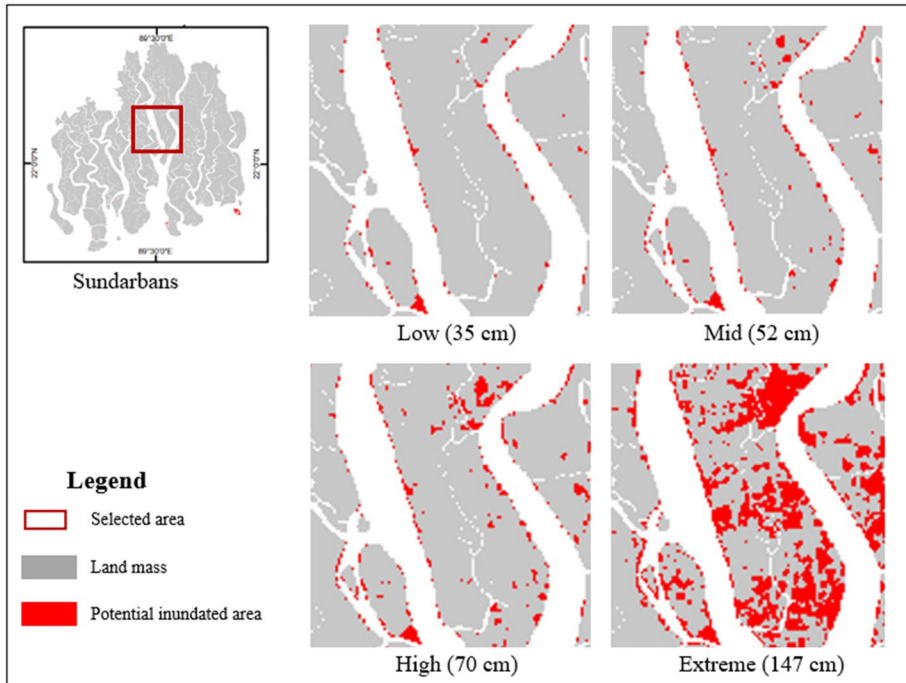

Fig. 8 Close-up (from our model) of the potential inundation areas for low, mid, high, and extreme SLR under −2.4 mm/year subsidence rate

also reported that the assumptions and results of a vast range of existing literature were likely to be incorrect. For instance, Loucks et al. (2010) projected that 96% of the Bangladesh Sundarbans will be reduced if SLR rises by 28 cm in 2070; this assumption seems too far in reality. The reason might be the DEM used in his study is not up to date or mistakes in the estimation of inundation. About 96% of Sundarbans areas will be inundated if SLR grows up to 3.5 m (Supplementary Fig. 2); however, it will take around 600 years with the current SLR (3.6 mm/year) (Fig. 3c) and net subsidence rate (−2.4 mm/year). Our results show that the potential inundation areas of the Sundarbans will not be the same as those earlier estimated by Payo et al. (2016) and Ghosh et al. (2019) by the end of the twenty-first century. Ghosh et al. (2019) estimated that the mangrove area is projected to be inundated by 26 km^2, 96 km^2, and 747 km^2 by the end of the twenty-first century for the low, mid, and extreme SLR scenarios, respectively, under the net subsidence rate of −2.4 mm/year. However, our study shows that the project inundation will be 40 km^2, 72 km^2, and 918 km^2 by the end of the twenty-first century with the same scenarios and subsidence rate. The different results might be that they used RCP 4.5 and 8.5 scenarios of West Bengal of India to find possible inundation of Bangladesh Sundarbans. However, the IPCC projection of SLR for West Bengal seems higher than the Bangladesh Sundarbans under the RCP 4.5 and 8.5 scenarios. A Hindu temple, about 400 years old, exists in the south Sundarbans, indicating that the combined effect of SLR and net subsidence is nominal (Steckler et al. 2022; Brammer 2014). The landmass of Sundarbans (i.e., offshore islands and sea-facing coastlines) is reducing significantly due to tidal surges and the soil erosion rate is much higher than the accretion (Akbar Hossain et al. 2022). Therefore, the SLR might not be the prime reason for the disappearance of the landmass of the Sundarbans.

Another factor that leads to inundation is related to cyclonic storms that cause coastal flooding. In this study, this factor was not considered as it is a seasonal event, and the inundation is not permanent. Storms and other compound effects are terribly important for risk studies, and this work can be a reference for future investigations on that topic.

5.3 Impact of future SLR scenarios and net subsidence

The results of our study depict that the potential inundation of the existing dense, moderate, and sparse forest areas will be not significant by the end of the twenty-first century for low, mid, and high SLR scenarios. The potential inundation of barren land areas is predicted to be higher than the dense, moderate, and sparse forest classes because most of the barren land covers the riverbanks and beaches (Supplementary Fig. 3) and lays in low elevation areas (Fig. 8). The permanent inundation of riverbanks and beaches increases the adjacent soil salinity and alters the successional path of mangroves. According to Ghosh et al. (2019), SLR associated with increased salinity replaces low-tolerant species with halo-tolerant coastal species, resulting in changing species composition. Regions with fast SLR and low sediment supply increase flooding, causing tree mortality at seaward mangrove margins and landward migration (Xie et al. 2022). The inundated areas for dense, moderate, and sparse forest classes tend to be higher under the extreme scenarios. However, the extreme scenario is not consistent for the Sundarbans regions. We justified the model using the station-based SLR rise data (1977 to 2020) of Sundarbans, which matches with the low (35 cm) SLR scenarios under a −2.4 mm/year subsidence rate. Therefore, SLR might not be a key factor in the degradation of Sundarbans. However, the other climate change-related hazards (e.g., cyclones, storm surges, salinity, soil erosion, pest and diseases) are the threats to the degradation of Sundarbans biodiversity, and its ecosystem (Mandal and Hosaka 2020; Gopal and Chauhan 2006).

Neogi et al. (2017) reported that the cyclonic storms increased by 26% from 1881 to 2001 towards the Sundarbans coastal area, resulting in long-term waterlog conditions, increasing soil salinity, and reducing biodiversity. Cyclone disturbances can cause significant damage to forest structures (Everham and Brokaw 1996) and forested landscapes (Foster and Boose 1992). The intensity of the tropical cyclonic damage is expected to be extremely high in the next few years (Alam and Dominey-Howes 2015; Moon et al. 2019; Ranson et al. 2014; Varotsos et al. 2015; Walsh et al. 2016).

Das and Datta (2016) reported that anthropogenic activities (e.g., shrimp farming, dam construction, and extensive extraction of forest resources) are one of the major causes of the ecological degradation of Sundarbans. For instance, upstream freshwater discharge from the Ganges River was reduced from 3700 m^3s^{-1} in 1962 to 364 m^3s^{-1} in 2006 due to the construction of the Farakka Barrage in 1975, rising the salinity level of the Sundarbans (Islam and Gnauck 2008). Moreover, the number of forest-dependent people adjacent to the Sundarbans is increasing, which may lead to a growing demand for forest resources (Ghosh et al. 2015) and a growing risk of over exploitation (Uddin et al. 2013) and ultimately for the integrity of Sundarbans ecosystems (Ahmed et al. 2021). According to the aforementioned studies, the SLR might not be a major cause of reducing the areas of the Sundarbans and its biodiversity. The SLR model of our study shows twelve potential inundations (Fig. 7) for the twenty-first century, and the level of inundation will not be a significant factor in changing the land cover class distribution. Ghosh et al. (2019) reported that the SLR would not only be a major cause of reducing the areas of Sundarbans mangrove vegetation through inundation by the end of the twenty-first century.

6 Conclusion

The study found many misconceptions that most of the Sundarbans areas will be inundated due to SLR by the end of the twenty-first century. The projection of future inundation due to SLR is greatly influenced by the DEM and subsidence rate. The present study followed appropriate methodological approaches regarding data collection, processing, and calculation.

The results of our model indicate that the projected landmass area to be inundated by 1%, 1.8%, 3.4%, and 23% in the twenty-first century for the low (35 cm), mid (52 cm), high (70 cm), and extreme (147 cm) SLR scenarios, respectively, under the current net subsidence rate of −2.4 mm/year. However, the extreme case scenario is not consistent for the Sundarbans regions. Projection of inundation level using the station-based SLR rise data (1977 to 2020) of Sundarbans matches with the low (35 cm) SLR scenarios under −2.4 mm/year subsidence rate. The low, mid, and high SLR will inundate the part of the river bank and beach areas. Therefore, the potential inundation due to SLR and its impact on the land cover areas will not be significant in the twenty-first century. However, the other climate change-related threats (e.g., cyclonic storms and soil erosion) and anthropogenic activities (e.g., agricultural expansion and industrialization) can be key reasons for the degradation of Sundarbans as they worsen the effects of SLR.

The findings of the present study might contribute to generating forest management strategies and achieving some goals of the Bangladesh Delta Plan (BDP) 2100. Moreover, the methodological approaches used in this study could help identify the future inundation level of the coastal areas due to SLR. However, DEM construction using the light detection and ranging (LiDAR) data provide higher accuracy, which is not available for

the Sundarbans. Therefore, further studies might use the LiDAR data to increase the DEM accuracy and other subsequent analysis. Furthermore, as the Sundarbans area is highly disturbed by anthropogenic activities, the spatial projection model of degradation might develop using the drivers of forest degradation.

Declarations

Ethics approval Not applicable

Consent to participate All authors consent to participate in the research.

Consent for publication All authors consent to submit the research findings.

Conflict of interest The authors declare no competing interests.

References

Ahmed A, Mahmud H, Sohel MSI (2021) DPSIR framework to analyze anthropogenic factors influence on provisioning and cultural ecosystem services of Sundarbans East Reserve Forest. Bangladesh Reg Stud Mar Sci 48:102042. https://doi.org/10.1016/j.rsma.2021.102042

Akbar Hossain K, Masiero M, Pirotti F (2022) Land cover change across 45 years in the world's largest mangrove forest (Sundarbans): the contribution of remote sensing in forest monitoring. Eur J Remote Sens 1–17. https://doi.org/10.1080/22797254.2022.2097450

Alam E, Dominey-Howes D (2015) A new catalogue of tropical cyclones of the northern Bay of Bengal and the distribution and effects of selected landfalling events in Bangladesh. Int J Climatol 35(6):801–835. https://doi.org/10.1002/joc.4035

Al-Nasrawi AKM, Kadhim AA, Shortridge AM, Jones BG (2021) Accounting for DEM error in sea level rise assessment within riverine regions; case study from the Shatt Al-Arab River Region. Environments 8(46). https://doi.org/10.3390/environments8050046

Anderson TR, Fletcher CH, Barbee MM, Romine BM, Lemmo S, Delevaux JMS (2018) Modeling multiple sea level rise stresses reveals up to twice the land at risk compared to strictly passive fooding methods. Sci Rep 8:14484. https://doi.org/10.1038/s41598-018-32658-x

Barlow ACD, Smith JLD, Ahmad IU, Hossain ANM, Rahman M, Howlader A (2011) Female tiger Panthera tigris home range size in the Bangladesh Sundarbans: the value of this mangrove ecosystem for the species conservation Fauna & Flora International. Oryx 45:125–128

Bera S, Chatterjee ND (2019) Mapping and monitoring of land use dynamics with their change hotspot in North 24-Parganas district, India: a geospatial- and statistical-based approach. Model Earth Syst Environ 5:1529–1551. https://doi.org/10.1007/s40808-019-00601-2

Brammer H (2014) Bangladesh's dynamic coastal regions and sea-level rise. Clim Risk Manag 1:51–62. https://doi.org/10.1016/j.crm.2013.10.001

Brown S, Nicholls R (2015) Subsidence and human influences in mega deltas: the case of the Ganges–Brahmaputra–Meghna. Sci Total Environ 527:362–374. https://doi.org/10.1016/j.scitotenv.2015.04.124

Chen CF, Son NT, Chang NB, Chen CR, Chang LY, Valdez M, Aceituno JL (2013) Multi-decadal mangrove forest change detection and prediction in Honduras, Central America, with Landsat imagery and a Markov chain model. Remote Sens 5(12):6408–6426. https://doi.org/10.3390/rs5126408

Colette A (2007) Case studies on climate change and World Heritage. UNESCO World Heritage Centre, Paris, France https://unesdoc.unesco.org/ark:/48223/pf0000150600

Das GK, Datta S (2016) Man-Made environmental degradation at Sunderbans. Reason-A Technical J 13:89–105. https://doi.org/10.21843/reas/2014/89-106/108127

Deb M, Ferreira M (2017) Potential impacts of the Sunderban mangrove degradation on future coastal flooding in Bangladesh. J Hydro-environment Res 17:30–46. https://doi.org/10.1016/j.jher.2016.11.005

Donato DC, Kauffman JB, Murdiyarso D, Kurnianto S, Stidham M, Kanninen M (2011) Mangroves among the most carbon-rich forests in the tropics. Nat Geosci 4(5):293–297. https://doi.org/10.1038/ngeo1123

Everham EM, Brokaw NV (1996) Forest damage and recovery from catastrophic wind. Bot Rev 62(2):113–185. https://doi.org/10.1007/BF02857920

FAO Forestry Economics and Policy Division (2010) Global forest resources assessment 2010: main report. Food and Agriculture Organization of the United Nations. Forestry Paper

Foster DR, Boose ER (1992) Patterns of forest damage resulting from catastrophic wind in central New England, USA. J Ecol 80(1):79–98. https://doi.org/10.2307/2261065

Gesch DB (2018) Best practices for elevation-based assessments of sea-level rise and coastal flooding exposure. Front Earth Sci 6:230. https://doi.org/10.3389/feart.2018.00230

Ghosh A, Schmidt S, Fickert T, Nüsser M (2015) The Indian Sundarban mangrove forests: history, utilization, conservation strategies and local perception. Diversity:149–169. https://doi.org/10.3390/d7020149

Ghosh MK, Kumar L, Langat PK (2019) Geospatial modelling of the inundation levels in the Sundarbans mangrove forests due to the impact of sea level rise and identification of affected species and regions. Geomat Nat Haz Risk 10(1):1028–1046. https://doi.org/10.1080/19475705.2018.1564373

Ghosh MK, Kumar L, Roy C (2016) Mapping long-term changes in mangrove species composition and distribution in the Sundarbans. Forests 7(12):305. https://doi.org/10.3390/f7120305

Giri C, Ochieng E, Tieszen LL, Zhu Z, Singh A, Loveland T, Masek J, Duke N (2010) Status and distribution of mangrove forests of the world using earth observation satellite data. Glob Ecol Biogeogr 20(1):154–159. https://doi.org/10.1111/j.1466-8238.2010.00584.x

Giri C, Pengra B, Zhu Z, Singh A, Tieszen LL (2007) Monitoring mangrove forest dynamics of the Sundarbans in Bangladesh and India using multi-temporal satellite data from 1973 to 2000. Estuar Coast Shelf Sci 73:91–100. https://doi.org/10.1016/j.ecss.2006.12.019

Gopal B, Chauhan M (2006) Biodiversity and its conservation in the Sundarban mangrove ecosystem. Aquat Sci 68(3):338–354. https://doi.org/10.1007/s00027-006-0868-8

Hawker L, Uhe P, Paulo L, Sosa J, Savage J, Sampson C, Neal J (2022) A 30 m global map of elevation with forests and buildings removed. Environ Res Lett 17:024016. https://doi.org/10.1088/1748-9326/ac4d4f

Islam MA, Paull DJ, Griffin AL, Murshed S (2020) Assessing ecosystem resilience to a tropical cyclone based on ecosystem service supply proficiency using geospatial techniques and social responses in coastal Bangladesh. Int J Dis Risk Reduction 49:1–17. https://doi.org/10.1016/j.ijdrr.2020.101667

Islam MM, Borgqvist H, Kumar L (2019) Monitoring Mangrove forest landcover changes in the coastline of Bangladesh from 1976 to 2015. Geocarto Int 34(13):1458–1476. https://doi.org/10.1080/10106049.2018.1489423

Islam MA, Mitra D, Dewan A, Akhter SH (2016) Coastal multi-hazard vulnerability assessment along the Ganges deltaic coast of Bangladesh- a geospatial approach. Ocean Coast Manag 127:1–5. https://doi.org/10.1016/j.ocecoaman.2016.03.012

Islam SN, Gnauck A (2008) Mangrove wetland ecosystems in Ganges-Brahmaputra delta in Bangladesh. Front Earth Sci China 2(4):439–448. https://doi.org/10.1007/s11707-008-0049-2

Jabir A, Hasan GMJ, Anam MM (2021) Correlation between temperature, sea level rise and land loss: an assessment along the Sundarbans coast. J King Saud Univ – Eng Sci. https://doi.org/10.1016/j.jksues.2021.07.012

Jevrejeva S, Grinsted A, Moore JC (2014) Upper limit for sea level projections by 2100. Environ Res Lett 9(10):104008. https://doi.org/10.1088/1748-9326/9/10/104008

Jones TG, Glass L, Gandhi S, Ravaoarinorotsihoarana L, Carro A, Benson L, Ratsimba HR, Giri C, Randriamanatena D, Cripps G (2016) Madagascar's mangroves: quantifying nation-wide and ecosystem specific dynamics, and detailed contemporary mapping of distinct ecosystems. Remote Sens 8(2):106. https://doi.org/10.3390/rs8020106

Kanniah KD, Sheikhi A, Cracknell AP, Goh HC, Tan KP, Ho CS, Rasli FN (2015) Satellite images for monitoring mangrove cover changes in a fast-growing economic region in southern Peninsular Malaysia. Remote Sens 7(11):14360–14385. https://doi.org/10.3390/rs71114360

Karim MF, Mimura N (2008) Impacts of climate change and sea-level rise on cyclonic storm surge floods in Bangladesh, Global Environ. Change 18:490–500. https://doi.org/10.1016/j.gloenvcha.2008.05.002

Kibria ASMG, Costanza R, Groves C, Behie AM (2018) The interactions between livelihood capitals and access of local communities to the forest provisioning services of the Sundarbans Mangrove Forest, Bangladesh. Ecosyst Serv 32:41–49. https://doi.org/10.1016/j.ecoser.2018.05.003

Kulp S, Strauss BH (2016) Global DEM errors underpredict coastal vulnerability to sea level rise and flooding. Front Earth Sci 4(36):1–8. https://doi.org/10.3389/feart.2016.00036

Kumar M, Mondal I, Pham QB (2021) Monitoring forest landcover changes in the Eastern Sundarban of Bangladesh from 1989 to 2019. Acta Geophys 69(29). https://doi.org/10.1007/s11600-021-00551-3

Levermann A, Winkelmann R, Nowicki S et al (2014) Projecting Antarctic ice discharge using response functions from SeaRISE ice-sheet models, Earth Syst. Dynam 5:271–293. https://doi.org/10.5194/esd-5-271-2014

Loucks C, Mayer SB, Hossain MAA, Barlow A, Chowdhury RM (2010) Sea level rise and tigers: predicted impacts to Bangladesh's Sundarbans mangroves: a letter. Clim Change 98:291–298. https://doi.org/10.1007/s10584-009-9761-5

Lovelock CE, Cahoon DR, Friess DA et al (2015) The vulnerability of Indo-Pacific mangrove forests to sea-level rise. Nature 526(7574):559–563. https://doi.org/10.1038/nature15538

Lu D, Weng Q (2007) A survey of image classification methods and techniques for improving classification performance. Int J Remote Sens 28:823–870. https://doi.org/10.1080/01431160600746456

Mandal MSH, Hosaka T (2020) Assessing cyclone disturbances (1988–2016) in the Sundarbans mangrove forests using Landsat and Google Earth Engine. Nat Hazards 102:133–150. https://doi.org/10.1007/s11069-020-03914-z

Moon IJ, Kim SH, Chan JC (2019) Climate change and tropical cyclone trend. Nature 570(7759):E3–E5. https://doi.org/10.1038/s41586-019-1222-3

Mukul SA, Alamgir M et al (2019) Combined effects of climate change and sea-level rise project dramatic habitat loss of the globally endangered Bengal tiger in the Bangladesh Sundarbans. Sci Total Environ 663:830–840. https://doi.org/10.1016/j.scitotenv.2019.01.383

Neogi SB, Dey M, Kabir SL, Masum SJH, Kopprio G, Yamasaki S, Lara R (2017) Sundarban mangroves: diversity, ecosystem services and climate change impacts. Asian J Med and Biol Res 2(4):488–507. https://doi.org/10.3329/ajmbr.v2i4.30988

Nishat B, Rahman AJMZ, Mahmud S (2019) Landscape narrative of the Sundarban: towards collaborative management by Bangladesh and India. http://documents.worldbank.org/curated/en/539771546853079693

Ortolano L, Sánchez-Triana E, Pau T, Ferdausi SA (2016) Managing the Sundarbans region: opportunities for mutual gain by India and Bangladesh. Int J Environ Sustain Dev 15(1):16–31. https://doi.org/10.1504/IJESD.2016.07333

Paszkowski A, Goodbred S, Borgomeo E et al (2021) Geomorphic change in the Ganges–Brahmaputra–Meghna delta. Nat Rev Earth Environ 2:763–780. https://doi.org/10.1038/s43017-021-00213-4

Payo A, Mukhopadhyay A, Hazra S, Ghosh T, Ghosh S, Brown S, Lázár AN (2016) Projected changes in area of the Sundarban mangrove forest in Bangladesh due to SLR by 2100. Clim Change 139:279–291. https://doi.org/10.1007/s10584-016-1769-z

Pham TD, Yoshino K (2015) Mangrove mapping and change detection using multi-temporal Landsat imagery in Hai Phong city, Vietnam. Paper presented at: The International Symposium on Cartography in Internet and Ubiquitous Environments Tokyo, Japan.

Poulter B, Halpin PN (2008) Raster modelling of coastal flooding from sea-level rise. Int J Geogr Inf Sci 22(2):167–182. https://doi.org/10.1080/13658810701371858

Quader MA, Agrawal S, Kervyn M (2017) Multi-decadal land cover evolution in the Sundarban, the largest mangrove forest in the world. Ocean Coast Manag 139:113–124. https://doi.org/10.1016/j.ocecoaman.2017.02.008

Rahman MM (2013) Temporal change detection of vegetation coverage in Patuakhali coastal area of Bangladesh Using GIS & Remotely Sensed Data. Int J Geomat Geosci 4(1):36–46

Rahman MM, Khan MNI, Hoque AF, Ahmed I (2015) Carbon stock in the Sundarban mangrove forest: spatial variations in vegetation types and salinity zones. Wetl Ecol Manag 23:269–283. https://doi.org/10.1007/s11273-014-9379-x

Ranson M, Kousky C, Ruth M, Jantarasami L, Crimmins A, Tarquinio L (2014) Tropical and extratropical cyclone damages under climate change. Clim Change 127(2):227–241. https://doi.org/10.1007/s10584-014-1255-4

Roy AKD, Alam K, Gow J (2013) Community perceptions of state forest ownership and management: a case study of the Sundarbans Mangrove Forest in Bangladesh. J Environ Manage 117:141–149. https://doi.org/10.1016/j.jenvman.2012.12.004

Sannigrahi S, Zhang Q, Pilla F, Joshi PK et al (2020) Responses of ecosystem services to natural and anthropogenic forcings: a spatial regression based assessment in the world's largest mangrove ecosystem. Sci Total Environ 715:137004. https://doi.org/10.1016/j.scitotenv.2020.137004

Steckler MS, Oryan B, Wilsonc CA et al (2022) Synthesis of the distribution of subsidence of the lower Ganges-Brahmaputra Delta. Bangladesh Earth-Sci Rev 224:103887. https://doi.org/10.1016/j.earscirev.2021.103887

Stehman SV (1996) Estimating the kappa coefficient and its variance under stratified random sampling. Photogramm Eng Remote Sens 62:401–407

Syvitski JPM, Kettner AJ et al (2009) Sinking deltas due to human activities. Nat Geosci 2(10):681–686. https://doi.org/10.1038/ngeo629

Uddin MS, Steveninck ER, Stuip M, Shah MAR (2013) Economic valuation of provisioning and cultural services of a protected mangrove ecosystem: a case study on Sundarbans Reserve Forest, Bangladesh. Ecosyst Serv 5:88–93. https://doi.org/10.1016/j.ecoser.2013.07.00

Vaglio Laurin G, Francini S, Luti T et al (2020) Satellite open data to monitor forest damage caused by extreme climate-induced events: a case study of the Vaia storm in Northern Italy. Forestry:Int J Forest Res. https://doi.org/10.1093/forestry/cpaa043

Varotsos CA, Efstathiou MN, Cracknell AP (2015) Sharp rise in hurricane and cyclone count during the last century. Theor Appl Climatol 119(3–4):629–638. https://doi.org/10.1007/s00704-014-1136-9

Walsh KJ, McBride JL, Klotzbach PJ, Balachandran S, Camargo SJ, Holland G, Knutson TR, Kossin JP, Lee T, Sobel A, Sugi M (2016) Tropical cyclones and climate change. Wiley Interdiscip Rev Clim Change 7(1):65–89. https://doi.org/10.1002/wcc.371

World Bank (2010) Economic of adaptation to climate change: Bangladesh, Volume 1. Main Report, Washington, DC https://openknowledge.worldbank.org/handle/10986/12837

World Bank (2000) Bangladesh: climate change and sustainable development. Report No. 21104, Dhaka, Bangladesh. http://hdl.handle.net/10986/15706

Xie D, Schwarz C, Kleinhans MG, Zhou Z, van Maanen B (2022) Implications of coastal conditions and sea-level rise on mangrove vulnerability: a bio-morphodynamic modeling study. J Geophys Res Earth 127:e2021JF006301. https://doi.org/10.1029/2021JF006301

Authors and Affiliations

Akbar Hossain Kanan[1] · **Francesco Pirotti[1,2]** · **Mauro Masiero[1]** · **Md Masudur Rahman[3]**

✉ Francesco Pirotti
  francesco.pirotti@unipd.it

  Akbar Hossain Kanan
  kanan.sust@gmail.com

  Mauro Masiero
  mauro.masiero@unipd.it

  Md Masudur Rahman
  rmasud@nmsu.edu

[1]   Department of Land, Environment, Agriculture and Forestry, University of Padova, Padova, Italy

[2]   CIRGEO Interdepartmental Research Center of Geomatics, University of Padova, Padova, Italy

[3]   Department of Geography, New Mexico State University, Las Cruces, USA